

# Evaluation of a self-amplifying mRNA reporter vaccine in explant models of broiler chickens

Janne Snoeck <sup>\*,†,2</sup>, Koen Chiers <sup>\*,\*</sup>, Ying Tam <sup>‡</sup>, Niek N. Sanders <sup>†,1</sup> and An Garmyn<sup>\*,1</sup>

<sup>\*</sup>Department of Pathobiology, Pharmacology and Zoological Medicine, Faculty of Veterinary Medicine, Ghent University, 9820 Merelbeke, Belgium; <sup>†</sup>Laboratory of Gene Therapy, Department of Veterinary and Biosciences, Faculty of Veterinary Medicine, Ghent University, 9820 Merelbeke, Belgium; and <sup>‡</sup>Acuitas Therapeutics, Vancouver, BC V6T 1Z3, Canada

**ABSTRACT** In order to minimize animal loss and economical loss, industrial poultry is heavily vaccinated against infectious agents. mRNA vaccination is an effective vaccination platform, yet little to no comprehensive, comparative studies in avians can be found. Nevertheless, poultry mRNA vaccination could prove to be very interesting due to the relatively low production cost, especially true when using self-amplifying mRNA (saRNA), and their extreme adaptability to new pathogens. The latter could be particularly useful when new pathogens join the stage or new variants arise. As a first step toward the investigation of saRNA vaccines in poultry, this study evaluates a luciferase-encoding saRNA in avian tracheal explants, conjunctival explants, primary chicken cecal cells and 18-day embryonated eggs. Naked saRNA in combination with RNase inhibitor and 2 different lipid-

based formulations, that is, ionizable lipid nanoparticles (LNPs) and Lipofectamine Messenger Max, were evaluated. The saRNA-LNP formulation led to the highest bioluminescent signal in the tracheal explants, conjunctival explants and cecal cell cultures. A dose-response experiment with these saRNA-LNPs (33–900 ng/well) in these avian organoids and cells showed a nonlinear dose-response relationship. After in ovo administration, the highest dose of the saRNA-LNPs (5 µg) resulted in a visual expression as a weak bioluminescence signal could be seen. The other delivery approaches did not lead to a visual saRNA expression in the embryos. In conclusion, effective entry of saRNA encapsulated in LNPs followed by successful saRNA translation in poultry was established. Hence, mRNA vaccination in poultry could be possible, but further in vivo testing is needed.

**Key words:** self-amplifying mRNA (saRNA), mRNA vaccination, lipid nanoparticle (LNP), administration route model, broiler chicken

2023 Poultry Science 102:103078  
<https://doi.org/10.1016/j.psj.2023.103078>

## INTRODUCTION

Poultry production is the fastest growing meat industry. It accounts for about half of the projected increase in total meat output. This can be attributed to its inherited lower real prices than other meat products due to the low purchase price of chickens, the small area of land needed to farm poultry, their rapid generation time, and their high productivity gains, which are increasing even further (Marangon and Busani, 2007; OECD/FAO, 2020). Hence, the poultry meat sector is predicted to expand by 16% by 2025 (OECD/FAO, 2016). Additionally, the poultry

sector focusing on egg production is expected to expand 14% by 2029 (OECD/FAO, 2020). In order to achieve this predicted growth, proper poultry health management is essential (Bagust, 2010; Abdul-Cader et al., 2018).

In an attempt to minimize or avoid the emergence of clinical infectious diseases at farm level, strict biosecurity measures and a busy poultry vaccination schedule are in place. Poultry are vaccinated (Baron et al., 2018) against infectious agents such as, for example, Newcastle Disease Virus (NDV), Infectious Bronchitis Virus (IBV), Infectious Bursal Disease Virus (IBDV), Marek's Disease Virus (MDV), and *Salmonella* sp. (Marangon and Busani, 2007; FAVV, 2019). Furthermore, continuous research into poultry vaccines is performed in order to reduce cost and to be prepared for the emergence of new disease strains including but not limited to the emerging transboundary highly pathogenic avian influenza strains (FAVV, 2019). This led to many vaccine trials involving genetic poultry vaccines and vector-based vaccines. This research resulted in the EMA

© 2023 The Authors. Published by Elsevier Inc. on behalf of Poultry Science Association Inc. This is an open access article under the CC BY-NC-ND license (<http://creativecommons.org/licenses/by-nc-nd/4.0/>).

Received May 4, 2023.

Accepted August 25, 2023.

<sup>1</sup>These authors contributed equally.

<sup>2</sup>Corresponding author: [janne.snoeck@ugent.be](mailto:janne.snoeck@ugent.be)

approval of multiple vector-based vaccines, using either Turkey Herpes Virus (**HVT**) or Fowlpox Virus (**FWPV**) as a vector against NDV, IBDV, Infectious Laryngotracheitis Virus (**ILTV**), and *Mycoplasma gallisepticum* (Romanutti et al., 2020).

However, more recently, the interest into mRNA vaccines soared to unprecedented heights due to the successful SARS-Cov2 mRNA vaccines designed by Pfizer/BioNTech and Moderna (Polack et al., 2020; Baden et al., 2021; Verbeke et al., 2021). mRNA vaccines can consist of either nonreplicating mRNA or self-amplifying mRNA (**saRNA**), also known as replicon RNA. While nonreplicating mRNA only encodes the antigen(s) of interest, self-amplifying mRNA also contains the coding sequences of all proteins required for RNA replication combined with a genomic and a subgenomic promoter (**SGP**) (Figure 1). Most often, these additional coding sequences have been derived from alphaviruses, either Venezuelan Equine Encephalitis Virus (**VEEV**), Sindbis virus, or Semliki Forest virus (Zhong et al., 2018). Their structural proteins are replaced with the genetic code of the antigen of interest, whereas the nonstructural proteins (**NSPs**), encoding the viral replicase complex consisting of helicase, RNA-dependent RNA polymerase,

capping, and polyadenylation enzymes, enable postadministration replication of the SG mRNA that encodes the antigen of interest (Zhong et al., 2018). Consequently, compared to conventional mRNA, equivalent levels of protection can be achieved using a reported 10- to 64-fold less material (Leyman et al., 2018; Vogel et al., 2018). Hence, the same dose of saRNA outperforms non-replicating mRNA (Leyman et al., 2018; Vogel et al., 2018). However, transfer of the mRNA vaccine to and into the cell greatly influences the antigen expression and strength of the immune response. Hence, many delivery vehicles, such as lipid nanoparticles (**LNPs**), polymer-based carriers, and lipopolyplexes were researched and optimized (Pardi et al., 2018; Zhong et al., 2018).

The interest in mRNA vaccines gained momentum because these vaccines have the potential for rapid, yet precise, development in a relatively cheaper way than traditional vaccines (Zhong et al., 2018; Feldman et al., 2019). Hence, these vaccines could be a great way to reduce the cost of the extensive poultry vaccination program and could be rapidly developed in order to combat the spread of, for example, highly pathogenic avian influenza virus strains to nonendemic regions (Feldman et al., 2019).

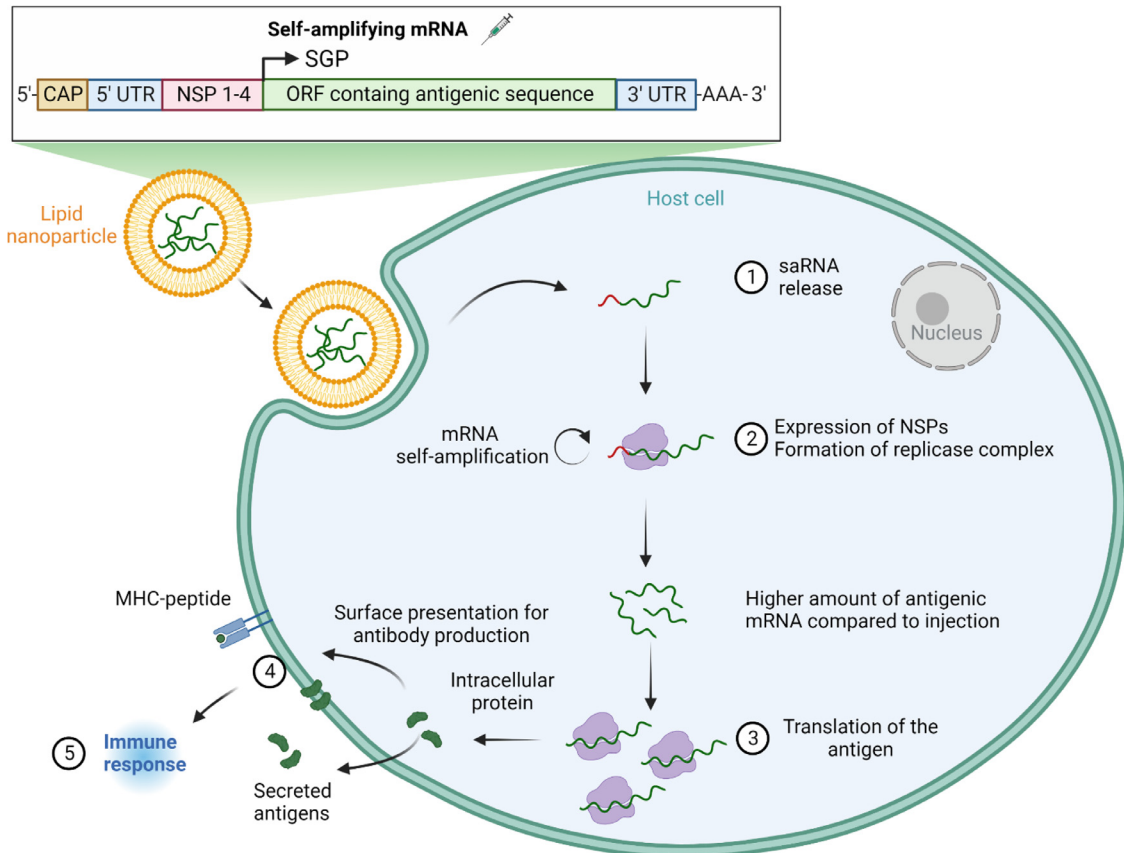


**Figure 1.** Schematic representation of the structure and mechanism of self-amplifying RNA. SaRNA consists of a capped 5' untranslated region (5' UTR), the mRNA sequence of 4 nonstructural proteins (NSPs) encoding the replicase complex, a subgenomic promoter (SGP), the open reading frame (ORF) encoding the protein/antigen of choice, a 3' UTR followed by a poly(A) tail. This saRNA is (1) released into the cytoplasm of the host cell. (2) The nonstructural proteins (NSPs) are translated and form the replicase complex. This complex is responsible for generating multiple negative sense RNA strands. These complementary strands serve as a template for the production of many copies of the original RNA strand. (3) These copies are then translated into the antigenic proteins. (4) The proteins are subsequently secreted or presented on the surface of the cell in order to elicit an (5) immune response resulting in either humoral or cellular immunity or both.

Unfortunately, as of yet, no structured, comparative research into poultry mRNA vaccines has been published.

This study focuses on *in vitro* investigation into the possible use and the most optimal administration route of saRNA vaccines in chickens using a model saRNA vaccine based on VEEV encoding the firefly luciferase 2 (**FLuc2**) reporter gene, allowing for visualization following luciferin administration.

## MATERIALS AND METHODS

### LNP-Formulated FLuc2-Encoding saRNA Vaccine Production

Self-amplifying mRNA (saRNA)-encoding FLuc2 was synthesized by *in vitro* transcription (IVT) from a linearized plasmid as previously described (Huysmans et al., 2019a). The plasmid is derived from VEEV strain TC-83 and contains the VEEV nonstructural proteins 1 till 4, the VEEV UTRs, promoter, and subgenomic promoter. A substitution in the 5' UTR (r.3a>g) and in nsP2 (p.Q739L) is present. The plasmid was amplified in *E. coli* DH5 $\alpha$  bacteria, which were cultivated in liquid broth (tryptone (10 g/L; VWR International, Leuven, Belgium), yeast extract (5 g/L; Invitrogen, Merelbeke, Belgium), sodium chloride (10 g/L; VWR International, Leuven, Belgium)) containing ampicillin (0.1 mg/mL; PanReac Applichem ITW reagents, Darmstadt, Germany). The plasmids were subsequently isolated using the Plasmid Plus Midi kit (QIAGEN, Hilden, Germany) and linearized by overnight incubation with the I-SceI restriction enzyme (New England Biolabs, Ipswich, MA). This linearized plasmid was used for IVT with the MEGAscript T7 Transcription kit (Life Technologies, Merelbeke, Belgium). Following IVT, the RNA was treated with DNase I (Invitrogen, Merelbeke, Belgium) and purified using the RNeasy Mini Kit (QIAGEN, Hilden, Germany). A cap1 structure was provided using the ScriptCap m7G Capping System (Cellscript, Madison, WI) and ScriptCap 2-O-Methyltransferase Kit (Cellscript, Madison, WI). The capped mRNA structure was once again purified using the RNeasy Mini kit (QIAGEN, Hilden, Germany). After the final purification, the saRNA was stored at -80°C. The integrity of the saRNA was analyzed using a previously described gel electrophoresis protocol (Aranda et al., 2012). SaRNA that passed the quality control was subsequently shipped to Acuitas Therapeutics (Vancouver, BC, Canada) for formulation into LNPs by microfluidic mixing of an ethanolic lipid solution with an aqueous sodium acetate buffer (pH 4) containing saRNA. Upon return, the saRNA-LNPs were visually inspected and no large aggregates were present. Subsequently, the functionality of said LNPs was evaluated by comparative transfection of HeLa cells against Lipofectamine Messenger Max (LMM) (2:1) (Thermo Fischer Scientific, Invitrogen, Merelbeke, Belgium). The mean size, polydispersity index, and zeta potential of the lipid-based saRNA nanoparticles dispersed in phosphate buffered saline

solution (PBS, pH 7.4) were determined using a Nano ZS90 (Malvern Pananalytical, Worcestershire, UK) and a NanoSight NS300 (NanoSight Ltd, Salisbury, UK). Calculations regarding these parameters employed a refractive index of 1.330 and a viscosity of 0.8872 mPa s.

### Isolation, Cultivation, and Transfection of Chicken Tracheal and Conjunctival Explants

Chicken tracheal and conjunctival explants were isolated from d 20 embryonated eggs from Ross 308 chickens (Hatchery Vervaeke-Belavi, Tielt, Belgium) according to the protocol of Reddy et al. (2016). The tracheal organ cultures (TOCs) were sliced into fine (circa 4 mm) o-rings, which were transferred to a 96-well plate. The conjunctival organ cultures were intact, in one piece, transferred to a 96-well plate. Both types of explants were cultivated for 16 d immersed in 200  $\mu$ L DMEM/F12 (Gibco, Waltham, MA) supplemented with 1% penicillin (Thermo Fischer Scientific, Merelbeke, Belgium), 1% streptomycin (Thermo Fischer Scientific, Merelbeke, Belgium), and 25 mM HEPES (pH 7.3) (Amresco, Solon, OH). Every 24 h, the explants were washed with PBS. Twenty-four hours postprelevation, the explants ( $n = 5$ ) were transfected with the FLuc2-encoding saRNA formulated with either Acuitas LNPs, liposomal LMM transfection reagent (2:1, meaning 2  $\mu$ L LMM was added to the formulation per  $\mu$ g saRNA) (Thermo Fischer Scientific, Merelbeke, Belgium) or unformulated (naked) saRNA plus 1 U/ $\mu$ L human placental RNase inhibitor (Promega Corporation, Madison, WI). The negative control consisted of RNase-free PBS (Invitrogen, Merelbeke, Belgium). Transfections occurred by adding 100 ng of formulated or not formulated saRNA in 20  $\mu$ L to the explants, which were submersed in 180  $\mu$ L DMEM/F12 culture medium. Next, transfection with an increasing amount of saRNA (30 ng, 50 ng, 100 ng, 300 ng, 500 ng, and 900 ng) using the most optimal delivery vehicle, that is, Acuitas LNPs, was performed. For each saRNA dose 5 explants were transfected. Transfection efficiency was quantified and visualized daily for 14 d by measuring the bioluminescent signal using the IVIS Illumina III (PerkinElmer, Zaventem, Belgium). In order to determine luciferase expression, 20  $\mu$ L 15 mg/mL D-luciferin (PerkinElmer, Zaventem, Belgium) was added to each explant cultivated in 180  $\mu$ L medium. No trypsinization was performed before analysis of the saRNA translation as the used luciferase substrate (D-luciferin) can freely move into tissues and cells. Each experiment was repeated in triplicate.

Transplant viability was assessed by daily microscopic monitoring of the ciliary beat in TOCs and by histological analysis of explants harvested either 3-days post-transfection (dPT), 7 dPT or at the endpoint of the visualization (14 dPT). To achieve this, the tracheal end conjunctival explants samples were collected and fixed in 4% neutral buffered formalin, embedded in paraffin, sectioned at 4  $\mu$ m (Microm HM360, Microm Inc.,

Hünstetten, Germany), dried during 1 h (60°C) and overnight (37°C). After dewaxing with xylene and rehydration in series with ethanol and distilled water, the sections were stained with hematoxylin and eosin (**H&E**) according standard techniques. To demonstrate apoptotic cells, sections were immunohistochemical labeled for caspase-3. In brief, slides were incubated in the pressure cooker with a citrate buffer (pH 6) for epitope exposure and peroxidase blocking was performed by incubating 5 min with Dako REAL Peroxidase-Blocking Solution (Agilent Technologies Inc., Santa Clara, CA). Slides were 30 min incubated with a polyclonal rabbit anti-caspase-3 antibody (ab4051; Abcam, Cambridge, UK) diluted (1/200) in antibody diluent (Agilent Technologies Inc., Santa Clara, CA). After washing, the sections were incubated (30 min) with the Dako REAL Envision+ System-HRP labeled polymer anti-rabbit (Agilent Technologies Inc., Santa Clara, CA). The slides were then washed 3 times in TBS and incubated at RT with 3,3'-diaminobenzidine (Agilent Technologies Inc., Santa Clara, CA) for 5 min. Sections were counterstained with hematoxylin followed by dehydration and mounting. External positive control for the immunohistochemical staining consisted of 4  $\mu\text{m}$  section of bursa samples from chickens. Internal controls consisted of normal endothelial cells in the examined tissues. No nonspecific staining was observed in any of the slides.

### Primary Cecal Cell Isolation, Cultivation, and Transfection

Ceca from D20 embryonated Ross 308 chicken eggs were used to isolate the primary epithelial crypt cells according to a modified protocol of Kim Van Deun and colleagues (Van Deun et al., 2008). The ceca were washed with Hank balances salt solution (**HBSS**) containing  $\text{Mg}^{2+}$  and  $\text{Ca}^{2+}$  (Gibco) in order to remove fecal content. Ceca are subsequently diced and digested overnight at 37°C in digestion medium (DMEM supplemented with 1% fetal bovine serum (**FBS**) (Biowest, Nuaille, France), 25  $\mu\text{g}/\text{mL}$  gentamicin (Gibco, Merelbeke, Belgium), 1% penicillin (Thermo Fischer Scientific, Merelbeke, Belgium), 1% streptomycin (Thermo Fischer Scientific, Merelbeke, Belgium), 375 U/mL collagenase (Sigma-Aldrich, Darmstadt, Germany) and 1 U/mL dispase (Roche, Vilvoorde, Belgium). The cells were centrifuged on a sorbitol gradient (30  $\times g$ , 5 min, 37°C) and seeded in a 24 well plate in 500  $\mu\text{L}$  cell medium (97.5% DMEM, 2.5% FBS, 10  $\mu\text{g}/\text{mL}$  insulin (Sigma-Aldrich, Darmstadt, Germany), 5  $\mu\text{g}/\text{mL}$  transferrin (Sigma-Aldrich, Darmstadt, Germany), 1.4  $\mu\text{g}/\text{mL}$  hydrocortisone (Sigma-Aldrich, Darmstadt, Germany) and 1  $\mu\text{g}/\text{mL}$  fibronectin (Sigma-Aldrich, Darmstadt, Germany), 1% penicillin and 1% streptomycin). The cells were transfected 24-h later (minimal surface coverage of 70–80%) similarly to the explants ( $n = 5$ ). The samples were transfected with Fluc2-encoding saRNA formulated with Acuitas LNPs, liposomal LMM transfection reagent (2:1) (Thermo Fischer Scientific,

Merelbeke, Belgium) or with unformulated (naked) saRNA plus 1 U/ $\mu\text{L}$  human placental RNase inhibitor (Promega Corporation, Madison, WI). As with the tracheal and conjunctival explants, we also investigated the transfection efficacy ( $n = 5$ ) as a function the saRNA dose (30 ng, 50 ng, 100 ng, 300 ng, 500 ng, and 900 ng) using the most optimal delivery vehicle, that is, LNPs. In both experiments, a negative control consisting of RNase-free PBS was included. Twenty-four hours post-transfection, 20  $\mu\text{L}$  15 mg/mL D-luciferin (PerkinElmer, Zaventem, Belgium) was added to 180  $\mu\text{L}$  trypsinized cells and the luciferase expression was quantified with the IVIS Illumina III. Due to the trypsinization step, only a single time point per sample could be measured. Cell viability was monitored by performing a WST-1 (water-soluble tetrazolium salt (4-[3-(4-iodophenyl)-2-(4-nitrophenyl)-2H-5-tetrazolio]-1,3-benzene disulfonate)) viability assay 24 h post-transfection. Twenty-microliter cell proliferation WST-1 reagent (Merck KGaA, Darmstadt, Germany) was added to 180  $\mu\text{L}$  loosened cells. After 30-min incubation, the absorbance at 450 nm (reference wavelength 660 nm) was measured using the EZ Read 400 Microplate reader (Biochrom Ltd., Cambridge, UK), after which the absorbance generated by the transfected cells was divided by the absorbance of the nontransfected control cells. After multiplication ( $\times 100\%$ ), cell viability percentage was obtained.

### In Ovo Transfection

Embryonated Ross 308 eggs were in ovo transfected at d 18 of incubation using 1  $\mu\text{g}$  of luciferase-encoding saRNA formulated with either LNPs or LMM transfection reagent. The in ovo saRNA doses were raised in order to maintain a similar RNA-to-fluid ratio compared to the ex vivo/in vitro experiments. The eggs contained circa 2 mL of amniotic fluid, whereas the wells only contained 200  $\mu\text{L}$ , resulting in a 10-fold dose increase. To that end, the egg shell was treated with 0.5% sodium hypochlorite solution in order to disinfect the egg shell. Subsequently, the egg shell was punctured using a disinfected (70% isopropanol) 18G needle and 100  $\mu\text{L}$  of the formulated FLuc2 saRNA was injected into the amniotic cavity through this puncture using a 22G needle (Figure 2). Using the most efficient formulation, that is, the LNPs, we studied 2 additional doses, that is, 0.5 and 5  $\mu\text{g}$ . PBS-treated embryonated eggs served as negative controls ( $n = 3$ ). Prior to the measurement, the top part of the shell was removed for optimal visualization. The bioluminescence signal was quantified every 12 h until hatch by subcutaneous injection of 100  $\mu\text{L}$  D-luciferin (150 mg/kg) (PerkinElmer, Zaventem, Belgium). Signal was measured with the IVIS Illumina III (PerkinElmer, Zaventem, Belgium). Viability was evaluated through hatching rate.

### Statistics

Statistical analyses were performed using GraphPad Prism software (version 8.4.3, GraphPad, San Diego,

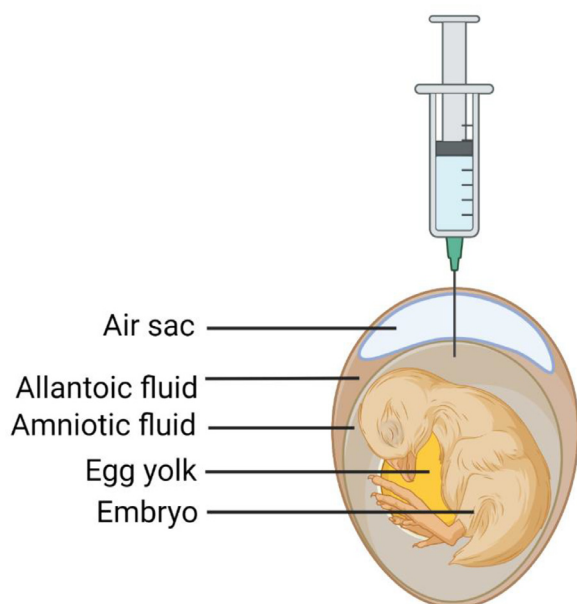


**Figure 2.** Visual representation of in ovo vaccination in an embryonated egg, during which the injection fluid is injected into the amniotic fluid.

CA). Luciferase expression in tracheal explants and conjunctival explants was analyzed using measurements every 24 h between 0 and 3 dPT ( $n/\text{treatment} = 5$ ) and subsequently between 0 and 7 dPT ( $n/\text{treatment} = 4$ ). Only the timespan between 0 and 7 dPT was considered in the analysis because little or no expression was visible after this point. Luciferase expression after in ovo injection was analyzed using measurements every 12 h between 0 and day of hatch. The average over time of the luciferase expression was analyzed using a fixed-effects model with the treatment group as fixed effect. Luciferase expression in primary chicken cecal cells was analyzed using measurements from a single timepoint (1 dPT). A 1-way analysis of variance (ANOVA) was carried out corrected for multiple comparisons (Tukey's multiple comparisons test). All tests were performed at a global 5% significant level. When comparing formulations, each group was compared against one another. When comparing doses, each dose was compared to the negative control. The data are represented as means  $\pm$  SD.

## RESULTS

### Physicochemical Properties of the saRNA Formulations

The mean hydrodynamic diameter of the nanoparticles that occurred after formulating the FLuc-2 saRNA with lipids and LMM transfection reagent was  $88.7 \text{ nm} \pm 16.4 \text{ nm}$  and  $166.3 \text{ nm} \pm 125.5 \text{ nm}$ , respectively. The polydispersity index (pdi) of the respective mixtures were  $0.137 \pm 0.016$  (LNPs) and  $0.710 \pm 0.104$  (LMM). The corresponding mean zeta potentials were  $-6.22 \text{ mV} \pm 0.4937 \text{ mV}$  (LNPs) and  $-35.2 \text{ mV} \pm 2.229 \text{ mV}$  (LMM).

### Luciferase Expression in Chicken Tracheal and Conjunctival Explants

In order to assess the prospects of an ocular or tracheal vaccine administration route in chickens, chicken tracheal and conjunctival explants were transfected with FLuc2-encoding saRNA formulated with either LNPs or LMM transfection reagent, and with naked, nonformulated FLuc2-encoding saRNA in the presence of a human placental RNase inhibitor ( $1 \text{ u}/\mu\text{L}$ ). Average over time analysis allowed us to estimate the total amount of protein produced during the full duration of the experiment. Additionally, a second transfection experiment was performed using different doses of LNP-formulated saRNA (33 ng, 50 ng, 100 ng, 300 ng, 500 ng, or 900 ng). The viability tests confirmed that the both types of explants were viable during the entire duration of the experiment, albeit a slight amount of apoptosis could be noted after 7 d of incubation. The number of apoptotic cells was somewhat higher 14 d after incubation, yet it was not enough to be solely responsible for the loss of luciferase expression.

The expression is visualized until d 7 post-transfection because little to no expression was visible after this point. Figures of the repeated experiments can be found in the supplemental data (Figures S1A and S2A (comparison of formulations); Figures S3A and S4A (comparison of concentrations)).

In the TOCs, the Acuitas saRNA-LNP-formulation outperformed the LMM reagent ( $P = 0.0003$ ) and the naked formulation ( $P = 0.0003$ ) (Figure 3A). The saRNA-LNP formulation resulted in the highest bioluminescent signal 2 dPT, followed by a gradual decrease. The expression level of the LMM group and the naked saRNA group did not differ significantly from the negative control (LMM:  $P = 0.9999$ ; naked saRNA:  $P = 0.9985$ ). However, the saRNA-LMM formulation generated a minor elevated expression after 24 h. After transfecting different doses of the LNP-encapsulated saRNA, nonlinear dose response characteristics could be seen. Initially from d 0 to 3 dPT, a dose of 100 ng, 300 ng, and 500 ng showed significantly different results (100 ng:  $P = 0.0018$ ; 300 ng:  $P = 0.0004$ ; 500 ng:  $P = 0.0397$ ). A dose of 300 ng LNP-formulated saRNA lead to the highest amount of total protein produced compared to the negative control (from 0 to 7 dPT:  $P = 0.0014$ ). Concentrations of 50 ng, 500 ng, and 900 ng per well showed no statistically significant results compared to the negative control (Figure 4A). Figures of the repeated experiments with tracheal explants can be found in the supplemental data (Figures S1A and S2A (comparison of formulations); Figures S3A and S4A (comparison of concentrations)).

Similar results were observed after transfection of the conjunctival explants (Figures 3B and 4B). Once again, the LNP-encapsulated saRNA resulted in the highest overall bioluminescent signal, peaking after 48 h and an expression that lasted for 1 wk. Surprisingly naked saRNA also resulted in clear although short-term (3 d) expression in the conjunctival explants that

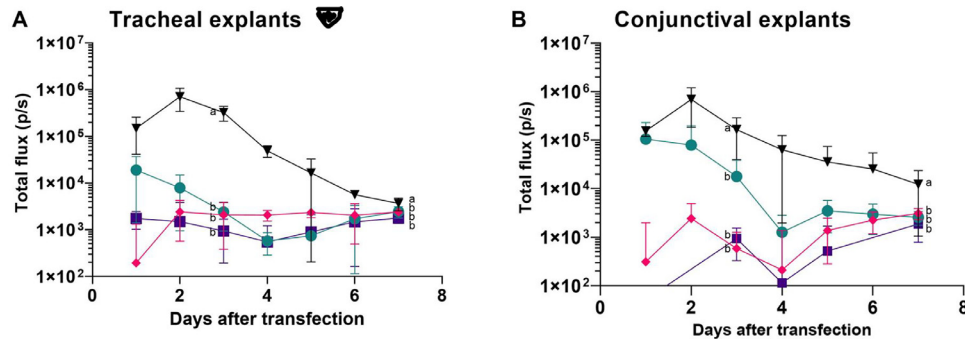


**Figure 3.** Luciferase expression (total flux in photons per second (p/s)) over time in tracheal explants (A) and conjunctiva explants (B) transfected with different Fluc-2 saRNA formulations (100 ng): saRNA encapsulated in lipid nanoparticles (saRNA-LNP formulation) ( $\blacktriangledown$ ) outperforms group Lipofectamine Messenger Max ( $\blacklozenge$ ), group naked saRNA ( $\bullet$ ) supplemented with RNase inhibitor and negative control group ( $\square$ ) containing only PBS. Treatments with different letter differ significantly from each other at the 5% global significance level. Hence, the saRNA-LNP formulation resulted in a luciferase expression that was significant higher than the 3 other formulations at both d 3 and 7.

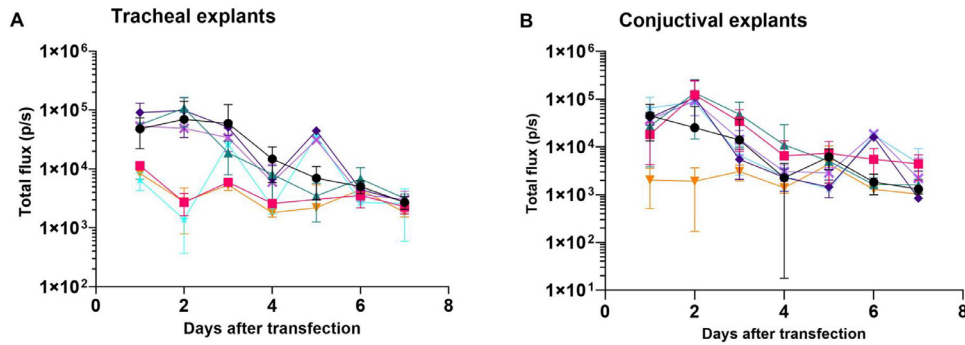


**Figure 4.** Luciferase expression (total flux in photons per second (p/s)) over time in tracheal explants (A) and conjunctival explants (B) transfected with 33 ng ( $\bullet$ ), 50 ng ( $\square$ ), 100 ng ( $\blacktriangle$ ), 300 ng ( $\blacklozenge$ ), 500 ng ( $\blackcross$ ) or 900 ng ( $\blackstar$ ) Fluc-2 saRNA encapsulated in lipid nanoparticles. Explants treated with only PBS served as negative controls ( $\blacktriangledown$ ).

outperformed the LMM-formulated saRNA by 2 orders of magnitude at d 1. The luciferase expression with the LMM formulation was similar to the negative control. The total amount of produced luciferase during the first 3 dPT was highest in the group treated with the LNP-formulated saRNA and was significantly different from the other included groups (negative control:  $P = 0.0005$ ; LMM:  $P = 0.0020$ ; naked saRNA:  $P = 0.0005$ ). This result persisted during the entire week (negative control:  $P = 0.0106$ ; LMM:  $P = 0.0282$ ; naked saRNA:  $P = 0.0108$ ). The dose-response curve of the LNP formulation was once again nonlinear (Figure 4B). Doses of 50 ng, 100 ng, and 300 ng saRNA resulted in a statistically significant amount of protein expression during the first 3 d after the transfection (50 ng:  $P = 0.0232$ ; 100 ng:  $P = 0.0193$ ; 300 ng:  $P = 0.0423$ ). Seven dPT, the results were variable. Figures of the repeated experiments with conjunctival explants can be found in the supplemental data (Figures S1B and S2B (comparison of formulations); Figures S3B and S4B (comparison of concentrations)).

### Luciferase Expression in Primary Cecal Chicken Cells

Oral vaccination is a very relevant route in poultry. Therefore, in this section, we investigated the saRNA

transfection efficacy in primary cecal chicken cells (PCCCs) as a representative of the digestive tract using the same formulations as the tracheal and conjunctival explants. One-day post-transfection with 100 ng naked or formulated FLuc-2 saRNA, the luciferase expression of the PCCC was measured (Figure 5). Figures of the repeated experiments can be found in the supplemental data (Figures S5 and S6). The Acuitas LNP-formulated saRNA showed a significantly higher expression than the negative control, the naked saRNA and the saRNA encapsulated in the LMM transfection reagent ( $P \leq 0.0001$  for each comparison). Using the LNPs we subsequently performed a dose-response experiments. Each Fluc-2 saRNA dose resulted in a clear expression that exceeded the background at least 3-fold (33 ng:  $P = 0.0025$ ; 50 ng:  $P = 0.0055$ ; 100 ng:  $P \leq 0.0001$ ; 300 ng:  $P \leq 0.0001$ ; 500 ng:  $P = 0.0001$ ; 900 ng:  $P = 0.0016$ ). Remarkably, all the doses resulted in a similar expression, albeit that the 100, 300, and 500 ng doses were slightly higher than the 33, 50, and 900 ng doses. Cell viability was confirmed by WST1-assay (Supplemental Figures S9 and S10). Cell viability data of the repeated experiments can be found in these figures as well. A clear but nonsignificant drop in viability was noticed when PCCCs were transfected with saRNA formulated in LFMM or naked saRNA plus RNase inhibitor. No change in cell viability was observed when PCCCs were transfected with saRNA-LNPs at all studied doses.

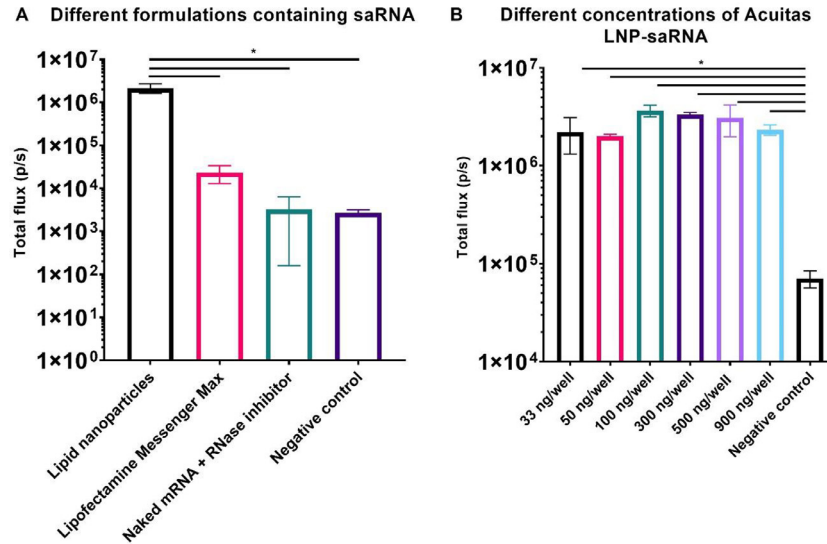


**Figure 5.** Comparison of luciferase expression (total flux in photons per second (p/s)) in primary chicken cecal cells (PCCC) transfected with different saRNA formulations (100 ng/well) (A) or different doses LNP-saRNA nanoparticles (C). Viability assays of both experiments are visualized in respectively Graph B and D. Data represent the mean and standard deviation of 5 replicates. Comparisons differing significantly at the 5% global significance level are represented by a single asterisk (\*).

**Luciferase Expression in Chicken Embryos After In Ovo Administration**

Eighteen-day embryonated eggs were injected in ovo (i.e., in the amniotic fluid) with 1 μg Fluc-2 saRNA formulated with Acuitas LNPs or LMM transfection reagent. Embryonated eggs treated with PBS served as negative controls. The saRNA-LNP formulation clearly outperformed the LMM transfection agent as the latter did not generate a bioluminescence signal that exceeded the background (Figure 6A), though admittedly, the bioluminescence emitted by the embryos was low. The expression usually arose near the beak of the chick, peaking through the membrane (Figure 7).

Next, different doses of luciferase-encoding saRNA encapsulated in Acuitas LNPs, either 0.5 μg, 1 μg, or 5 μg, were injected in ovo (Figure 6B). As observed in the explants and the primary cecal cells, the 3 saRNA doses did not generate a clear difference in expression in the embryos. Overall, 92% of the eggs hatched, ensuring the viability of the embryos.

Figures of the repeated experiments can be found in the supplemental data (Figures S7 and S8).

**DISCUSSION**

The efficacy of a vaccine depends on numerous aspects such as its immunogenicity, the choice of antigen, the vaccination schedule and the route of application (Kembi et al., 1995; Steitz et al., 2010; Pardi et al., 2015; Leigh et al., 2018). For practical reasons in terms of mass application, vaccination in poultry occurs often by use of a whole body spray, administration through drinking water or in ovo application. This study looked into the possibilities of administration of saRNA vaccines in poultry, employing a luciferase-encoding saRNA using tracheal and conjunctival explant models, primary cecal chicken cells and in ovo administration in embryonated eggs, which mimic the mentioned administration routes. The ex vivo explant cultures are more suitable to predict the outcome of possible in vivo experiments compared to traditional cell cultures, as most of the 3-dimensional structures and cell-cell interactions are not altered. Additionally, in vivo studies are more and more contested due to ethical reasons.

Whole body spray vaccination mainly serves to target the respiratory route and is delivered to the eyes, nares

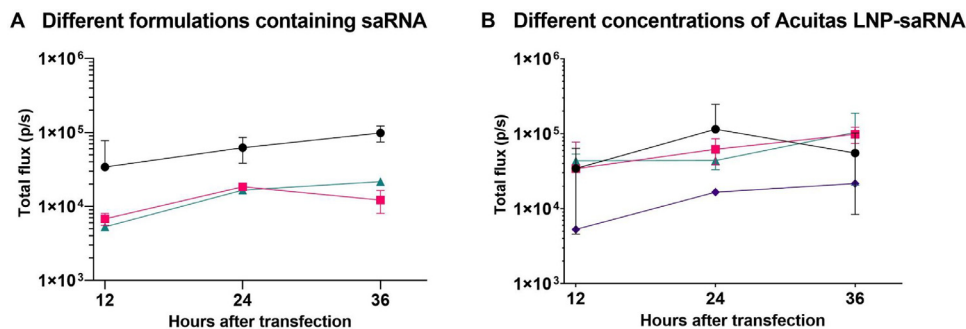


**Figure 6.** Luciferase expression (total flux in photons per second (p/s)) over time after in ovo injection of 18-day embryonated eggs with (A) 1 μg Fluc-2 saRNA formulated with lipid nanoparticles (LNPs) (●) or Lipofectamine Messenger Max (□) and (B) different doses LNP-formulated-saRNA (5 μg (●), 1 μg (□), 0.5 μg (◆)). As negative control embryonated eggs were in ovo injected with PBS (▲).

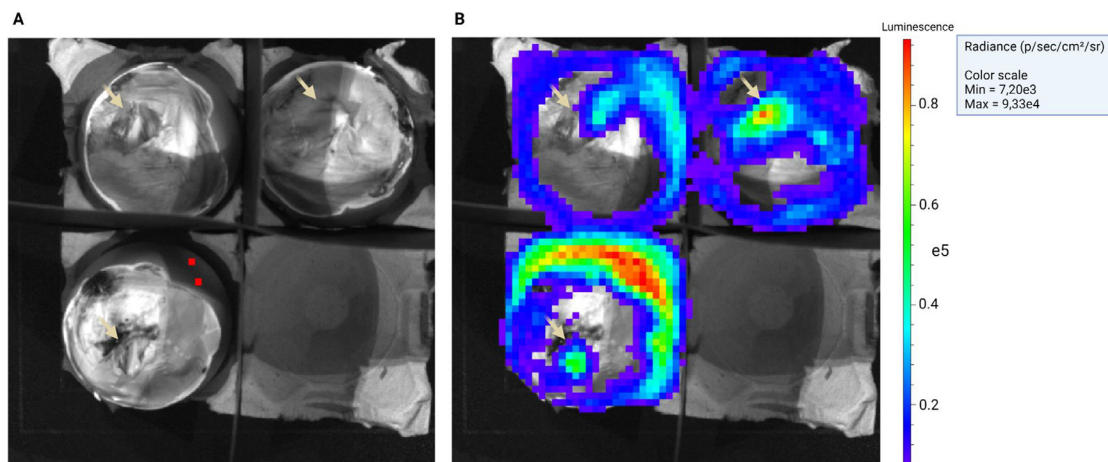


**Figure 7.** IVIS read-out of the in ovo experiment ( $5 \mu\text{g}$ ) 36-h postinjection. Figure A shows a photograph of the eggs showing the beaks of the embryo's (arrows) peeking through the membrane. Figure B shows the visualization of the bioluminescent signal. The expression is clearly visible near the beak of the embryo's. Egg shell background signal can also be noticed.

and in the oral cavity through preening activities (Leigh et al., 2018). To mimic this route, tracheal and conjunctival explants were used. In the past, the TOC system (Jones and Hennion, 2008) has been successfully used for characterization of the early immune responses induced by AIV (Reemers et al., 2009), the isolation of avian bronchitis virus (Cook et al., 1976), the investigation into persistent NDV infections (Cummiskey et al., 1973), the cultivation of oocysts or sporozoites of *Cryptosporidium baileyi* (Zhang et al., 2012) and investigation into the replication characteristics of infectious laryngotracheitis virus in mucosal tissues (Reddy et al., 2014). This last study also employed the conjunctival explants. Furthermore the conjunctival explants were also used by Darbyshire et al. (1976) in order to investigate the pathogenicity and infection efficiency of avian infectious bronchitis virus.

To our knowledge, gut explants are not available. Hence, we opted to use chicken primary cecal cell cultures (Cook et al., 1976) to simulate the oral administration route, as this route targets the intestinal tract. These cultures have been used to investigate the influence of arabinosyloligosaccharides (Eeckhaut et al., 2008) and butyric acid (Van Immerseel et al., 2004) on shedding and colonization of *Salmonella* Enteritidis and the colonization of *Campylobacter jejuni* in the chicken gut (Van Deun et al., 2008).

After transfecting the explants and the PCCCs, a clear bioluminescent signal caused by the expressed luciferase could be discerned. In all 3 models, the Acuitas LNPs resulted in the highest expression levels. Hence, the saRNA can successfully enter the cells and be translated. This leads to believe that RNA administration via spray or drinking water could lead to expression in the conjunctiva, trachea and/or gastrointestinal tract provided that formulation can reach the adequate transfection site unscathed. Both spray and oral vaccination have their own difficulties. Spray vaccination could be hampered by tracheal mucus production, yet this was no problem during the transfection of the explants. The low pH in the gastrointestinal tract and the presence of

lipase in the gut could prove to be a hurdle for oral vaccination. However, oral administration of an LNP-formulated saRNA vaccine, albeit using the sequence of RNA-dependent RNA polymerase as found in a norovirus instead of the NSPs of an alphavirus, against SARS-CoV-2 in mice showed high expression of the S-protein in the small intestine and a lower amount of expression in the large intestine (Keikha et al., 2021).

LNPs have proven to be efficient carriers for several types of nucleic acids (siRNA, nucleoside-modified mRNA, saRNA) and effectively deliver them to the tissues (Pardi et al., 2015; McKay et al., 2020; Polack et al., 2020; Baden et al., 2021). The use of liposomes as a delivery carrier of small molecules has been approved by the FDA for the first time in 1995 (Doxil) and in 2018, the first LNP-siRNA therapeutic, Onpattro, was approved by both FDA and EMA (Gopalakrishna, 2014; Akinc et al., 2019). LNP-mRNA vaccines against SARS-CoV-2 were the first LNP-mRNA vaccines to receive FDA and EMA approval (Polack et al., 2020; Baden et al., 2021). LNPs are typically composed of ionizable lipids, phospholipids, sterols (most of the time cholesterol), and lipid-anchored polyethylene-glycols (PEG), which have an important influence on the size of the particles and prevent aggregation during storage (Hassett et al., 2021; Schoenmaker et al., 2021; Verbeke et al., 2021). LNPs are usually produced using a microfluidic system. This microfluidics system consists of an aqueous acidic buffer phase containing the saRNA and a solvent, ethanol, containing the dissolved lipids. These 2 phases are mixed by injecting them laminarly, ensuring slow mixing into a common tube, during which the ionizable lipid, which turns positive in the presence of the aqueous acidic buffer, is able to form a complex with the negatively charged saRNA. Due to the change in polarity, the orientation of the other lipids changes, making them align their hydrophobic tails, enclosing the complexed saRNA, resulting in a LNP encapsulating the saRNA. Then, the pH of the solvent is changed to 7.4, in order to safely inject the vaccine into living organisms (Belliveau et al., 2012).

Composition-wise, it is noteworthy that current 2 COVID-19 mRNA vaccines employ LNPs as a delivery vehicle. Additionally, the composition of both LNP types is remarkably similar, differing only in ionizable lipid. ALC-0315 (a proprietary Acuitas lipid) and SM-102 are respectively utilized as an ionizable lipid in the Pfizer/BioNTech and the Moderna vaccine and are structurally very similar (Polack et al., 2020; Baden et al., 2021).

Besides the lipid composition, the size and zeta potential are important physicochemical properties of mRNA-LNPs as well. Ideally, they are less than 100 nm and have a close to neutral surface charge in order to allow trafficking to lymphoid tissue and be taken up by the necessary cells (No Authors Listed, 2021). Transfection with naked saRNA only proved successful in the conjunctival explants, not in the TOCs or the PCCCs. Even if some previous studies demonstrated the ability of naked mRNA to be expressed in cell cultures (Lorenz et al., 2011) and in live animals (Huysmans et al., 2019a), the efficacy of naked mRNA was usually increased by electroporation (Leyman et al., 2018; Huysmans et al., 2019a,b). The lack of expression using the naked saRNA in the TOCs and PCCCs could be caused by degeneration of the RNA before translation can occur, as RNases are ubiquitous in bodily fluids. Yet, the RNase inhibitor has proven to prevent this degradation at least to a certain degree (Huysmans et al., 2019a). Another reason for the lack of measurable translation is the inability of the RNA to enter the cell. Due to its hydrophilicity, high molecular weight, and negative charge, mRNA has poor cellular uptake in its free form (Baptista et al., 2021) and depends on endocytic routes. It is possible that in the conjunctiva other endocytic routes are active that allow cytoplasmic delivery of low amounts of intact naked saRNA (Qaddoumi et al., 2003).

The luciferase expression of the LNP-formulated saRNA showed nonlinear dose-response characteristics. Over all, a dose of 300 ng per well (24-well plates) seemed most optimal in case of the explants. The capacity of the lower doses, that is, 33 ng/well, to result in a total flux that was only slightly below that of statistically significant doses is remarkable and most likely due to the self-amplifying capacity of the saRNA. The drop in luciferase expression at the highest dose (i.e., 900 ng/well) is probably due to activation of the innate immune system by a saRNA mediated triggering of the pattern recognition receptors, such as oligodendylate synthetase and RNA-dependent protein kinase (PKR) (Linares-Fernandez et al., 2020). Once activated, PKR phosphorylates eukaryotic initiation factor-2, leading to the inhibition of translation and OAS helps activate RNase L, which degrades non-self-RNA (Chakrabarti et al., 2011; Linares-Fernandez et al., 2020). Both immune reactions lead to a decreased presence of the administered replicating RNA.

When transfecting PCCCs with the Acuitas LNP-saRNA nanoparticles, each tested saRNA dose resulted in luciferase translation that was more or less the same

for each dose. This again shows a nonlinear dose-response relationship. It is possible that the range of doses was not broad enough. Another possible explanation is that saturation of the uptake of the LNP-saRNA nanoparticles or the limits of the translational capacity of the transfected cells was reached (Pardi et al., 2015). Unfortunately, due to the short lifespan of the PCCCs, it could not be visualized if the higher doses resulted in an extended duration of luciferase expression.

When evaluating the in ovo vaccination route, naked saRNA combined with an RNase inhibitor was not included as this group did not produce favorable results in the explants and the PCCCs. Moreover, inclusion of electroporation in the protocol was not possible due to the egg shell and the difficult reachability of the embryo. In ovo administration of the LNP-formulated luciferase-encoding saRNA generated a visible bioluminescence signal. However, the emitted light signal was not significantly higher than the background. Nonetheless, several side notes have to be made. First, the IVIS Illumina III measures surface bioluminescent light generated by the expressed luciferase. Tissues scatter and absorb light. Hence bioluminescent light sources positioned deeper in the tissue are difficult to detect. This means that only the bioluminescent light from the part of the embryo that is visible from the top of the egg can be measured. Second, the feathers can also efficiently block the bioluminescent light. Third, in ovo vaccination aims to inject the vaccine directly in the amniotic fluid (Ricks et al., 1999; Wakenell et al., 2002; Avakian, 2006). However, a small percentage of the injections occurs in the embryo. Without opening the egg, it is impossible to determine whether the injection occurs in the amniotic fluid or subcutaneously in the embryo itself. If the LNP-saRNA nanoparticles are injected into the embryo, expression will occur locally, near the injection spot, which makes it hard to detect such local bioluminescent signal in a living, growing, and moving embryo. If the saRNA-LNP formulation is injected in the amniotic fluid, expression may be more ubiquitous as the embryo will absorb the amniotic fluid intraocular, intranasal or by ingesting it. Hence, luciferase may be expressed by the internal structures, which complicates the detection of the bioluminescent light using the IVIS Illumina III as tissues decrease and scatter the emitted bioluminescent signal. Nevertheless, in some cases, a small amount of luciferase generated light could be visualized when the beak started breaking through the shell membrane (Figure 6). A more sensitive detection of the delivered saRNA in the different tissues of the embryo's or chickens could be obtained using quantitative RT-PCR (Vervaeke et al., 2022). The latter can complement the bioluminescent imaging data.

During protocol optimization, it became clear that the top of the egg shell prevented adequate measurement (data not shown). Removal of the top part of the egg shell could possibly compromise the embryo viability as the embryo is not optimally protected. However, this does not seem to negatively influence the viability of the embryos as the hatch rate in the LNP-saRNA-treated

embryonated eggs was 92%, which is higher than the reported industrial average of 90% (Archer, 2013). Our experiments indicate that the in ovo vaccination route could still be a successful administration route for mRNA vaccination in poultry.

Over all, these results show a trend toward mRNA vaccination in chickens to be feasible. Initial field testing of a viral pseudoparticle vaccine containing a RNA replicon backbone encoding the H5 of H5N8 avian influenza showed favorable results in ducks (Niqueux et al., 2023). Although the latter RNA replicon vaccine cannot be considered as a real synthetic saRNA vaccine as it uses a viral particle for its delivery, it underlines that our saRNA-LNP vaccine will most likely result in an effective synthetic mRNA vaccine platform against infectious diseases in birds in general and in poultry in particular. In order to elucidate the possible applications or uses of mRNA in poultry, further in vivo assessments are necessary.

In conclusion, in vitro transfection of tracheal and conjunctival explants and primary chicken cecal cells results in luciferase expression, ensuring effective entry into avian cells and successful saRNA translation in poultry is possible. The results are most favorable if the saRNA is formulated in LNPs. The dose-titration of the LNP-saRNA displays a nonlinear dose-response relationship and hence cannot directly be extrapolated to live animals. Visualization of in ovo vaccination on an in vitro level, while the embryo was inside the egg shell, proved a difficult predictor for in vivo in ovo vaccination. In order to elucidate these applications, further in vivo research is needed, yet these results point toward promising in vivo applications for mRNA vaccination.

## ACKNOWLEDGMENTS

Delphine Ameye and Joachim Christiaens for histological technical assistance. Sarah Loomans for technical assistance IHC. This project was funded by Bijzonder onderzoeksfonds (BOF) of Ghent University (grant numbers BOFST2019004601 and BOF.BAS.2018.0028.01).

## DISCLOSURES

We have no conflicts of interest to disclose.

## SUPPLEMENTARY MATERIALS

Supplementary material associated with this article can be found in the online version at doi:10.1016/j.psj.2023.103078.

## REFERENCES

- Abdul-Cader, M. S., V. Palomino-Tapia, A. Amarasinghe, H. Ahmed-Hassan, U. De Silva Senapathi, and M. F. Abdul-Careem. 2018. Hatchery vaccination against poultry viral diseases: potential mechanisms and limitations. *Viral Immunol.* 31:23–33.
- Akinc, A., M. A. Maier, M. Manoharan, K. Fitzgerald, M. Jayaraman, S. Barros, S. Ansell, X. Du, M. J. Hope, T. D. Madden, B. L. Mui, S. C. Semple, Y. K. Tam, M. Ciufolini, D. Witzgmann, J. A. Kulkarni, R. van der Meel, and P. R. Cullis. 2019. The Onpattro story and the clinical translation of nanomedicines containing nucleic acid-based drugs. *Nat. Nanotechnol.* 14:1084–1087.
- Aranda, P. S., D. M. LaJoie, and C. L. Jorcyk. 2012. Bleach gel: a simple agarose gel for analyzing RNA quality. *Electrophoresis* 33:366–369.
- Archer, G. S. C. 2013. Incubating and hatching eggs. *Texas A&M Agrilife Extension* 1:1–11.
- Avakian, A. P. 2006. Understanding in ovo vaccination. *Int. Hatchery Pract.* 20:15–17.
- Baden, L. R., H. M. El Sahly, B. Essink, K. Kotloff, S. Frey, R. Novak, D. Diemert, S. A. Spector, N. Rouphael, C. B. Creech, J. McGettigan, S. Khetan, N. Segall, J. Solis, A. Brosz, C. Fierro, H. Schwartz, K. Neuzil, L. Corey, P. Gilbert, H. Janes, D. Follmann, M. Marovich, J. Mascola, L. Polakowski, J. Ledgerwood, B. S. Graham, H. Bennett, R. Pajon, C. Knightly, B. Leav, W. Deng, H. Zhou, S. Han, M. Ivarsson, J. Miller, T. Zaks, and C. S. Group. 2021. Efficacy and safety of the mRNA-1273 SARS-CoV-2 vaccine. *N. Engl. J. Med.* 384:403–416.
- Bagust, T. 2010. Poultry health and disease control in developing countries. *Poultry Development Review*.
- Baptista, B., R. Carapito, N. Laroui, C. Pichon, and F. Sousa. 2021. mRNA, a Revolution in Biomedicine. *Pharmaceutics* 13:2090, doi:10.3390/pharmaceutics13122090.
- Baron, M. D., M. Iqbal, and V. Nair. 2018. Recent advances in viral vectors in veterinary vaccinology. *Curr. Opin. Virol.* 29:1–7.
- Belliveau, N. M., J. Huft, P. J. Lin, S. Chen, A. K. Leung, T. J. Leaver, A. W. Wild, J. B. Lee, R. J. Taylor, Y. K. Tam, C. L. Hansen, and P. R. Cullis. 2012. Microfluidic synthesis of highly potent limit-size lipid nanoparticles for In vivo delivery of siRNA. *Mol. Ther. Nucleic Acids* 1:e37.
- Chakrabarti, A., B. K. Jha, and R. H. Silverman. 2011. New insights into the role of RNase L in innate immunity. *J. Interferon Cytokine Res.* 31:49–57.
- Cook, J. K., J. H. Darbyshire, and R. W. Peters. 1976. The use of chicken tracheal organ cultures for the isolation and assay of avian infectious bronchitis virus. *Arch. Virol.* 50:109–118.
- Cummiskey, J. F., J. V. Hallum, M. S. Skinner, and G. A. Leslie. 1973. Persistent Newcastle disease virus infection in embryonic chicken tracheal organ cultures. *Infect. Immun.* 8:657–664.
- Darbyshire, J. H., J. K. Cook, and R. W. Peters. 1976. Organ culture studies on the efficiency of infection of chicken tissues with avian infectious bronchitis virus. *Br. J. Exp. Pathol.* 57:443–454.
- Eeckhaut, V., F. Van Immerseel, J. Dewulf, F. Pasmans, F. Haesebrouck, R. Ducatelle, C. M. Courtin, J. A. Delcour, and W. F. Broekaert. 2008. Arabinosyloligosaccharides from wheat bran inhibit Salmonella colonization in broiler chickens. *Poult. Sci.* 87:2329–2334.
- FAVV. 2019. Newcastle disease. Accessed June 2021. <https://www.favv-afscab.be/animalhealth/newcastledisease/>.
- Feldman, R. A., R. Fuhr, I. Smolenov, A. Mick Ribeiro, L. Panther, M. Watson, J. J. Senn, M. Smith, Ö. Almarsson, H. S. Pujar, M. E. Laska, J. Thompson, T. Zaks, and G. Ciaramella. 2019. mRNA vaccines against H10N8 and H7N9 influenza viruses of pandemic potential are immunogenic and well tolerated in healthy adults in phase 1 randomized clinical trials. *Vaccine* 37:3326–3334.
- Gopalakrishna, P. 2014. Nanomedicines for cancer therapy: an update of FDA approved and those under various stages of development. *SOJ Pharm. Pharm. Sci.* 1:13.
- Hassett, K. J., J. Higgins, A. Woods, B. Levy, Y. Xia, C. J. Hsiao, E. Acosta, Ö. Almarsson, M. J. Moore, and L. A. Brito. 2021. Impact of lipid nanoparticle size on mRNA vaccine immunogenicity. *J. Control Release* 335:237–246.
- Huysmans, H., J. De Temmerman, Z. Zhong, S. Mc Cafferty, F. Combes, F. Haesebrouck, and N. N. Sanders. 2019a. Improving the repeatability and efficacy of intradermal electroporated self-replicating mRNA. *Mol. Ther. Nucleic Acids* 17:388–395.
- Huysmans, H., Z. Zhong, J. De Temmerman, B. L. Mui, Y. K. Tam, S. Mc Cafferty, A. Gitsels, D. Vanrompay, and N. N. Sanders. 2019b. Expression kinetics and innate immune response after electroporation and LNP-mediated delivery of a

- self-amplifying mRNA in the skin. *Mol. Ther. Nucleic Acids* 17:867–878.
- Jones, B. V., and R. M. Hennion. 2008. The preparation of chicken tracheal organ cultures for virus isolation, propagation, and titration. *Methods Mol. Biol.* 454:103–107.
- Keikha, R., S. M. Hashemi-Shahri, and A. Jebali. 2021. The evaluation of novel oral vaccines based on self-amplifying RNA lipid nanoparticles (saRNA LNPs), saRNA transfected *Lactobacillus plantarum* LNPs, and saRNA transfected *Lactobacillus plantarum* to neutralize SARS-CoV-2 variants alpha and delta. *Sci. Rep.* 11:21308.
- Kembi, F. A., O. O. Delano, and M. A. Oyekunle. 1995. Effect of three different routes of administration on the immunogenicity of infectious bursal disease vaccine. *Rev. Elev. Med. Vet. Pays Trop.* 48:33–35.
- Leigh, S. A., J. D. Evans, S. D. Collier, and S. L. Branton. 2018. The impact of vaccination route on *Mycoplasma gallisepticum* vaccine efficacy. *Poult. Sci.* 97:3072–3075.
- Leyman, B., H. Huysmans, S. Mc Cafferty, F. Combes, E. Cox, B. Devriendt, and N. N. Sanders. 2018. Comparison of the expression kinetics and immunostimulatory activity of replicating mRNA, nonreplicating mRNA, and pDNA after intradermal electroporation in pigs. *Mol. Pharm.* 15:377–384.
- Linares-Fernandez, S., C. Lacroix, J. Y. Exposito, and B. Verrier. 2020. Tailoring mRNA vaccine to balance innate/adaptive immune response. *Trends Mol. Med.* 26:311–323.
- Lorenz, C., M. Fotin-Mleczek, G. Roth, C. Becker, T. C. Dam, W. P. Verdurmen, R. Brock, J. Probst, and T. Schlake. 2011. Protein expression from exogenous mRNA: uptake by receptor-mediated endocytosis and trafficking via the lysosomal pathway. *RNA Biol.* 8:627–636.
- Marangon, S., and L. Busani. 2007. The use of vaccination in poultry production. *Rev. Sci. Technol.* 26:265–274.
- McKay, P. F., K. Hu, A. K. Blakney, K. Samnuan, J. C. Brown, R. Penn, J. Zhou, C. R. Bouton, P. Rogers, K. Polra, P. J. C. Lin, C. Barbosa, Y. K. Tam, W. S. Barclay, and R. J. Shattock. 2020. Self-amplifying RNA SARS-CoV-2 lipid nanoparticle vaccine candidate induces high neutralizing antibody titers in mice. *Nat. Commun.* 11:3523.
- Niqueux, E., M. Flodrops, C. Allee, M. O. Lebras, I. Pierre, K. Louboutin, C. Guillemoto, A. Le Prioux, S. Le Bouquin-Leneveu, A. Keita, M. Amelot, C. Martenot, P. Massin, M. Cherbonnel-Pansart, F. X. Briand, A. Schmitz, C. Cazaban, G. Dauphin, T. Delquigny, S. Lemiere, J. M. Watier, M. Mogler, I. Tarpey, B. Grasland, and N. Eterradossi. 2023. Evaluation of three hemagglutinin-based vaccines for the experimental control of a panzootic clade 2.3.4.4b A(H5N8) high pathogenicity avian influenza virus in mule ducks. *Vaccine* 41:145–158.
- No Authors Listed. 2021. Let's talk about lipid nanoparticles. *Nat. Rev. Mater.* 6:99, doi:10.1038/s41578-021-00281-4.
- OECD/FAO. 2016. OECD-FAO, Agricultural Outlook 2016-2025. OECD Publishing, Paris, France.
- OECD/FAO. 2020. OECD-FAO Agricultural Outlook 2020-2029. OECD Publishing, Paris, France.
- Pardi, N., M. J. Hogan, F. W. Porter, and D. Weissman. 2018. mRNA vaccines - a new era in vaccinology. *Nat. Rev. Drug Discov.* 17:261–279.
- Pardi, N., S. Tuyishime, H. Muramatsu, K. Kariko, B. L. Mui, Y. K. Tam, T. D. Madden, M. J. Hope, and D. Weissman. 2015. Expression kinetics of nucleoside-modified mRNA delivered in lipid nanoparticles to mice by various routes. *J. Control Release* 217:345–351.
- Polack, F. P., S. J. Thomas, N. Kitchin, J. Absalon, A. Gurtman, S. Lockhart, J. L. Perez, G. Perez Marc, E. D. Moreira, C. Zerbini, R. Bailey, K. A. Swanson, S. Roychoudhury, K. Koury, P. Li, W. V. Kalina, D. Cooper, R. W. Frenck Jr., L. L. Hammitt, O. Tureci, H. Nell, A. Schaefer, S. Unal, D. B. Tresnan, S. Mather, P. R. Dormitzer, U. Sahin, K. U. Jansen, W. C. Gruber, and C. C. T. Group. 2020. Safety and efficacy of the BNT162b2 mRNA Covid-19 vaccine. *N. Engl. J. Med.* 383:2603–2615.
- Qaddoumi, M. G., H. J. Gukasyan, J. Davda, V. Labhasetwar, K. J. Kim, and V. H. Lee. 2003. Clathrin and caveolin-1 expression in primary pigmented rabbit conjunctival epithelial cells: role in PLGA nanoparticle endocytosis. *Mol. Vis.* 9:559–568.
- Reddy, V. R., L. Steukers, Y. Li, W. Fuchs, A. Vanderplasschen, and H. J. Nauwynck. 2014. Replication characteristics of infectious laryngotracheitis virus in the respiratory and conjunctival mucosa. *Avian Pathol.* 43:450–457.
- Reddy, V. R., I. Trus, L. M. Desmarests, Y. Li, S. Theuns, and H. J. Nauwynck. 2016. Productive replication of nephropathogenic infectious bronchitis virus in peripheral blood monocyte cells, a strategy for viral dissemination and kidney infection in chickens. *Vet. Res.* 47:70.
- Reemers, S. S., M. J. Groot Koerkamp, F. C. Holstege, W. van Eden, and L. Vervelde. 2009. Cellular host transcriptional responses to influenza A virus in chicken tracheal organ cultures differ from responses in in vivo infected trachea. *Vet. Immunol. Immunopathol.* 132:91–100.
- Ricks, C. A., A. Avakian, T. Bryan, R. Gildersleeve, E. Haddad, R. Ilich, S. King, L. Murray, P. Phelps, R. Poston, C. Whitfill, and C. Williams. 1999. In ovo vaccination technology. *Adv. Vet. Med.* 41:495–515.
- Romanutti, C., L. Keller, and F. A. Zanetti. 2020. Current status of virus-vectored vaccines against pathogens that affect poultry. *Vaccine* 38:6990–7001.
- Schoenmaker, L., D. Witzigmann, J. A. Kulkarni, R. Verbeke, G. Kersten, W. Jiskoot, and D. J. A. Crommelin. 2021. mRNA-lipid nanoparticle COVID-19 vaccines: structure and stability. *Int. J. Pharm.* 601:120586.
- Steitz, J., R. A. Wagner, T. Bristol, W. Gao, R. O. Donis, and A. Gambotto. 2010. Assessment of route of administration and dose escalation for an adenovirus-based influenza A virus (H5N1) vaccine in chickens. *Clin. Vaccine Immunol.* 17:1467–1472.
- Van Deun, K., F. Pasmans, R. Ducatelle, B. Flahou, K. Vissenberg, A. Martel, W. Van den Broeck, F. Van Immerseel, and F. Haesebrouck. 2008. Colonization strategy of *Campylobacter jejuni* results in persistent infection of the chicken gut. *Vet. Microbiol.* 130:285–297.
- Van Immerseel, F., J. De Buck, I. De Smet, F. Pasmans, F. Haesebrouck, and R. Ducatelle. 2004. Interactions of butyric acid- and acetic acid-treated *Salmonella* with chicken primary cecal epithelial cells in vitro. *Avian Dis.* 48:384–391.
- Verbeke, R., I. Lentacker, S. C. De Smedt, and H. Dewitte. 2021. The dawn of mRNA vaccines: the COVID-19 case. *J. Control Release* 333:511–520.
- Vervaeke, P., S. E. Borgos, N. N. Sanders, and F. Combes. 2022. Regulatory guidelines and preclinical tools to study the biodistribution of RNA therapeutics. *Adv. Drug. Deliv. Rev.* 184:114236.
- Vogel, A. B., L. Lambert, E. Kinnear, D. Busse, S. Erbar, K. C. Reuter, L. Wicke, M. Perkovic, T. Beissert, H. Haas, S. T. Reece, U. Sahin, and J. S. Tregoning. 2018. Self-amplifying RNA vaccines give equivalent protection against influenza to mRNA vaccines but at much lower doses. *Mol. Ther.* 26:446–455.
- Wakenell, P. S., T. Bryan, J. Schaeffer, A. Avakian, C. Williams, and C. Whitfill. 2002. Effect of in ovo vaccine delivery route on herpesvirus of turkeys/SB-1 efficacy and viremia. *Avian Dis.* 46:274–280.
- Zhang, S., F. Jian, G. Zhao, L. Huang, L. Zhang, C. Ning, R. Wang, M. Qi, and L. Xiao. 2012. Chick embryo tracheal organ: a new and effective in vitro culture model for *Cryptosporidium baileyi*. *Vet. Parasitol.* 188:376–381.
- Zhong, Z., M. Séan, F. Combes, H. Huysmans, J. De Temmerman, A. Gitsels, D. Vanrompay, J. Portela Catani, and N. Sanders. 2018. mRNA therapeutics deliver a hopeful message. *Nano Today* 23:16–39.